

DT-MRI DATA VISUALISATION USING THE DUAL TREE COMPLEX WAVELET TRANSFORM

Nick Kingsbury, Argyris Zymnis *

Alonso Pena †

Cambridge University Engineering Department
Signal Processing Group
Trumpington Street
Cambridge, CB2 1PZ, UK

Department of Radiology and
Academic Neurosurgery Unit
Cambridge University
Cambridge, CB2 2QQ, UK

ABSTRACT

In this paper a novel visualisation method for diffusion tensor MRI datasets is introduced. This is based on the use of Complex Wavelets in order to produce “stripy” textures which depict the anisotropic component of the diffusion tensors. Grey-scale pixel intensity is used to show the isotropic component. This paper also discusses enhancements of the technique for 3D visualisation.

1. INTRODUCTION

Diffusion Tensor MRI (DT-MRI) is a relatively new medical imaging method which permits the visualisation of white matter brain structures *in vivo*. It involves the calculation of the diffusion of water along different directions, which is described by a 3x3 symmetric and positive definite tensor. This directionality property allows the DT-MRI data to be used in a technique called “tractography” to reconstruct white matter fibre tracts within the brain.

Using matrix algebra, it is possible to reduce the dimensionality of the tensor and to obtain several scalar and vector measures of diffusion. These include various weighted quantities involving the tensor’s eigenvectors and eigenvalues. Several authors have proposed ways of visualising the DT-MRI data using these measures [1], [2], [3]. What is of particular importance is the measure of the isotropic and anisotropic component of diffusion at each voxel. By isotropic, we term the component of diffusion which is equal in all directions and by anisotropic we term the measure of diffusion which is concentrated on one dominant direction.

In this study we first briefly introduce some common methods of tensor visualisation. We then proceed to propose a novel method which makes use of the Dual Tree Complex Wavelet Transform (DT-CWT) [4], [5]. The algorithm we have developed produces images which show

both the isotropic and the anisotropic component in a way that makes it easy for the human eye to interpret. This can also follow fibre tracts in 2D with high accuracy and computational efficiency.

2. METHOD

2.1. DT-MRI Data Visualisation

A DT-MRI dataset consists of a specified number of slices of the brain with a given resolution. We used a dataset consisting of 8 slices (each 10mm apart) with resolution 128x128 and with intervoxel spacing 1mm. Each voxel consists of a 2nd order Cartesian tensor, whose elements represent the diffusion gradient of water along different directions, as shown in equation (1).

$$\mathbf{D} = \begin{pmatrix} D_{xx} & D_{xy} & D_{xz} \\ D_{yx} & D_{yy} & D_{yz} \\ D_{zx} & D_{zy} & D_{zz} \end{pmatrix} \quad (1)$$

This tensor is symmetric along its main diagonal and is also positive definite, as negative diffusion (negative eigenvalues) has no physical meaning. Hence this tensor has six degrees of freedom plus the positive definite constraint.

In order to reduce the dimensionality of the data, each tensor is diagonalised. A computationally efficient way of diagonalising a DT-MRI dataset is demonstrated in [6]. The resulting sorted eigenvalues and eigenvectors can be used to obtain measures of the isotropy and anisotropy within the dataset. A useful way of representing the tensor is as a 3-dimensional ellipsoid whose 3 principal axes are defined by the tensor’s eigenvectors scaled by their corresponding eigenvalues. In this sense, the voxels can be classified into three main categories: isotropic or spherical (when all eigenvalues are approximately equal), anisotropic or cigar-like (when one eigenvalue is distinctly larger than the other two) and finally flying saucer-like (when one eigenvalue is distinctly smaller than the other two). The latter case is very rare in DT-MRI.

*Supported by the Trinity College Summer Research Studentship scheme

†Thanks to the Wellcome Trust for a fellowship in Mathematical Biology

In the existing DT-MRI literature [3], [2], the most common quantities used when analysing diffusion tensor data are the mean diffusion (\bar{D}) defined as:

$$\bar{D} = \frac{1}{3} \text{tr}(\mathbf{D}) = \frac{\lambda_1 + \lambda_2 + \lambda_3}{3} \quad (2)$$

where “tr” represents the trace of the tensors and $\lambda_1 > \lambda_2 > \lambda_3$ are the sorted eigenvalues, and the fractional anisotropy (FA), defined as:

$$FA = \sqrt{\frac{3}{2}} \frac{\sqrt{(\lambda_1 - \bar{D})^2 + (\lambda_2 - \bar{D})^2 + (\lambda_3 - \bar{D})^2}}{\sqrt{\lambda_1^2 + \lambda_2^2 + \lambda_3^2}} \quad (3)$$

In our analysis we will instead use three alternative quantities to characterise the diffusion tensors, which we will term the isotropic component (X_{is}) and the anisotropic component (X_{an}) defined as:

$$X_{is} = \frac{\lambda_2 + \lambda_3}{2} \quad (4)$$

$$|X_{an}| = \lambda_1 - X_{is} \quad (5)$$

$$\vec{X}_{an} = |X_{an}| \times \vec{e}_1 \quad (6)$$

where \vec{e}_1 , \vec{e}_2 and \vec{e}_3 are the tensor’s eigenvectors. Note that the polarity of the eigenvectors is arbitrary.

There is an existing method of vector visualisation. This involves creating an rgb image in which the red, green and blue image components are the absolute value of the x,y and z vector components of \vec{X}_{an} respectively [2], but we now propose an improvement on this.

2.2. Use of the Complex Wavelet Transform

After obtaining X_{is} and X_{an} , the problem of visualising the DT-MRI data is equivalent to the problem of visualising a vector field along with a scalar function on the same plot. The DT-CWT is well suited to do this, due to its good directional selectivity [4], [5]. Other transforms, such as curvelets, could have been used, but the particular characteristics of the DT-CWT make it well suited to this application.

Figure 1 shows the impulse response of the six different directional subbands available at each level of the DT-CWT. It can be clearly seen that these take the form of stripes pointing in the direction θ_d of the specific subband (i.e. at $\pm 15^\circ$, 45° , 75°). The DT-CWT can normally be used to analyse any given image in terms of its directional components (edges) at each orientation.

We can hence generate a scalar “stripy” image which is a representation of the vector field. This can be done by calculating the components of the vectors along the different subband orientations and exciting the subbands of an inverse DT-CWT by a suitable amount. Furthermore, if we include a scalar field as the scaling function in the inverse DT-CWT, we can superimpose the “stripiness” on the smooth grey levels, representing the scalar values.



Fig. 1. Impulse responses of different directional subbands in the DT-CWT

The equation which we use to get the component of each CWT subband from each vector \vec{X}_{an} is:

$$\vec{X}_{an} = X\mathbf{i} + Y\mathbf{j} + Z\mathbf{k} \quad (7)$$

$$\theta_X = \arctan \frac{Y}{X} \quad (8)$$

$$\phi_d = \theta_X - \theta_d \quad (9)$$

$$X_d = \begin{cases} |X_{an}| \times \cos^2(2\phi_d) & , \text{if } |\phi_d| < 45^\circ, \\ 0 & , \text{otherwise.} \end{cases} \quad (10)$$

$$W_{d,i} = X_d \times e^{(\alpha + \theta_{lag})j} \quad (11)$$

where ϕ_d is the angle formed between each vector and the direction of excitation of a particular subband d and $W_{d,i}$ is the resulting wavelet coefficient at subband d and point i . Note that a squared cosine is used, and the angle ϕ_d is doubled in order to make the excitation of the subbands more directionally selective. This rule was found to give a good tradeoff between selectivity and interpolation as a function of θ_x .

The angle α is a random variable uniformly distributed in the range 0 to 2π . This angle is the same for all $W_{d,i}$ with same i but different d (i.e. all wavelet coefficients originating from the same vector but belonging to different directional subbands).

By looking at figure 1 it can be seen that the impulse responses for different CWT subbands are not aligned. This means that the peak for each impulse response does not occur at the same point. Since proper alignment of the stripes is needed, a phase lag has to be added to the CWT inputs in order to align all the responses. This phase lag is different for each CWT subband and was calculated experimentally. This is denoted as θ_{lag} in equation 11.

The fact that we initially use random phases for all wavelet coefficients causes many of the stripes not to line up. One way of tackling this is to iteratively apply the forward and inverse CWT, by exciting the subbands such that the magnitude of all wavelet coefficients is kept constant to the initial calculated value, but the phase of the wavelet coefficients is the phase after the previous iteration. It was found experimentally that this process causes the resulting inverse CWT image to have stripes which are more aligned to each other. This is due to the fact that the DT-CWT is a redundant transform. Thus there is overlap between adjacent basis functions in the CWT domain. This means that if we move from the spatial domain back to the CWT domain,

the phases of wavelet coefficients in adjacent subbands will tend to be “pulled” into alignment. If we also apply the magnitude constraint discussed above, we can achieve an improved alignment of the stripes.

It was found experimentally that after 5 or 6 iterations of the above process good alignment of the stripes is achieved¹. In this iterative algorithm we have only used a 1 level inverse and forward CWT in order to reduce computational load. For the final iteration however, we apply a 2-level inverse CWT to get a higher resolution result. The finer level has six completely empty subbands and the coarser level is computed as described above. This is done in order to increase the size of the image by 4 and make the stripes more easily discernible.

Figure 2 shows the result of applying the above algorithm with 5 iterations on the fourth slice of our dataset. The stripes are lined up quite well and they give a good representation of the horizontal fibre tracts within the brain. Grey-scale intensity represents isotropic diffusion, while “stripiness” represents horizontal anisotropic diffusion.

It can be noted that there are regions within the image where the stripes seem to have random directions. In these regions the vector field has a large vertical component and thus a good way of representing this vertical information is needed.

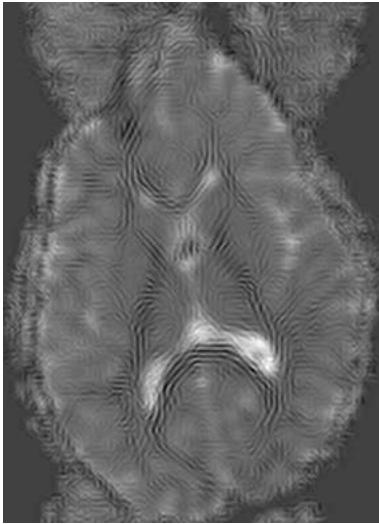


Fig. 2. “Stripy” representation of the fourth slice of the dataset

2.3. Representation of Vertical Information

We decided to show the vertical component in two ways.

Firstly, a red-scale image for each slice is generated, which represents the vertical component of each principal eigenvector. This is added to the grey-scale isotropic intensity image and hence we can show both quantities simultaneously.

¹Unless the initial random phase causes stripes to be in antiphase

Secondly we decided to represent stripes with a vertical direction, by using a chequer-board stripy pattern. This is done by superimposing stripes which are perpendicular to the stripes calculated in the previous sub-section. The amount of perpendicular stripes added to the parallel ones depends on the angle between the principal eigenvector and the horizontal plane. If this angle is 0° then no perpendicular stripes are added. If this angle is 90° the amount of parallel and perpendicular stripes is equal and hence the stripes do not convey any horizontal directional information. The amount of parallel and perpendicular “stripiness” is given by two gain factors: G_h (for parallel stripes) and G_v for perpendicular stripes. This is shown in the following formula:

$$\vec{e}_1 = x\mathbf{i} + y\mathbf{j} + z\mathbf{k} \quad (12)$$

$$\theta_{vert} = \arctan \frac{z}{\sqrt{x^2 + y^2}} \quad (13)$$

$$G_h = \cos \frac{\theta_{vert}}{2} \times |X_{an}| \quad (14)$$

$$G_v = \sin \frac{\theta_{vert}}{2} \times |X_{an}| \quad (15)$$

The Gain factors G_h and G_v are multiplied with unit vectors in a parallel and normal direction (respectively) to the direction of the horizontal components. These are then separately fed into the algorithm, instead of X_{an} described in the previous sub-section. The resulting images are added, together with the grey-scale image representing isotropic diffusion and the red-scale image representing vertical anisotropic diffusion. An example of this technique, as applied to the fourth slice of our dataset is shown in figure 3.

As can be seen the proposed method can generate medical images which are easy to interpret. The “stripy” patterns give a very fine detail of the directionality of the white matter tracts. This is especially good in the region of the brain cortex, in the so-called “association fibers”, joining adjacent sulci. The low amplitude stripes near the cortical surface (skull boundary) show that relatively small anisotropies can be observed quite clearly. This is not the case with the rgb image shown in figure 4. This shows a distinct advantage of our method in terms of offering complementary information which facilitates the visualisation of the 3D diffusion tensor.

3. EXTENDING THE METHOD TO 3D

We have shown how to use our visualisation method to present DT-MRI data in 2D. If we want to extend this method into three dimensions, we must first find a good way to interpolate between existing slices of our dataset.

The obvious way of doing this is to iteratively perform simple averaging of the tensor elements between adjacent slices. The big problem with this method is that it will blur the interpolated image.

We can instead take advantage of the anisotropic components of the 3D tensors in the dataset. This requires find-

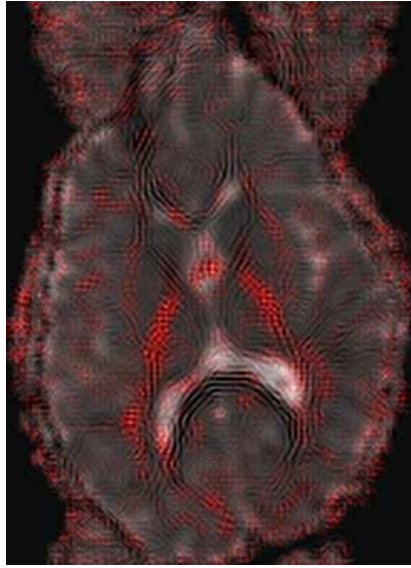


Fig. 3. Representation of the fourth slice of the dataset with vertical information

ing a pair of voxels in adjacent slices, whose principal eigenvector points to the same voxel in the interpolated slice. Having found this pair of voxels we then compute its eigenvalues and eigenvectors as some form of weighted mean of the eigenquantities of the top and bottom voxels. If no two vectors line up properly for a given interpolated voxel, we can just perform a least squared error calculation in its neighborhood. This technique is currently under development.

The final aim of this project is to extend the existing method into 3D. The 3D DT-CWT has 28 subbands distributed on the surface of a hemisphere and their impulse responses generate directional planar-like structures. In order to generate filament-like structures, we need to excite two subbands whose planes of impulse response are perpendicular to each other and to a given anisotropic vector.

This is quite a challenging task. It requires efficient computer memory management and a good grasp of 3D CWT visualisation and forms the remaining part of this project.

4. CONCLUSIONS

We have presented a novel way of visualising DT-MRI data based on the use of the dual tree CWT. This method is easy to implement, it is computationally efficient and it produces images which are easy to physically interpret.

5. ACKNOWLEDGEMENTS

The authors would like to thank Professor J. D. Pickard, Dr. A. Carpenter, Dr. J. H. Gillard and Dr. R. Tasker at Addenbrooke's Hospital, Cambridge University for their invaluable help in this project.

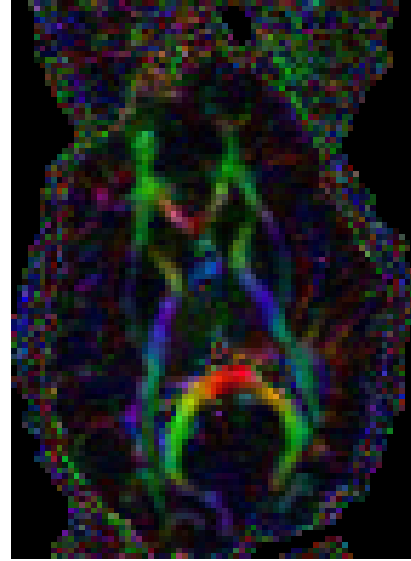


Fig. 4. Representation of the DT-MRI data using the standard rgb technique, where red is x, green is y, blue is z

6. REFERENCES

- [1] C. F. Westin, S. Maier, H. Mamata, A. Nabavi, F. A. Jolesz, and R. Kikinis, "Processing and visualisation for diffusion tensor MRI," *Medical Image Analysis*, vol. 6, pp. 93–108, 2002.
- [2] Y. Masutani, S. Aoki, O. Abe, N. Hayashi, and K. Otomo, "MR diffusion tensor imaging: recent advance and new techniques for diffusion tensor visualisation," *European Journal of Radiology*, vol. 46, pp. 53–66, 2003.
- [3] A. Pena, H. A. Green, T. A. Carpenter, J. D. Pickard, and G. H. Gillard, "Enhanced visualisation and quantification of magnetic resonance diffusion tensor imaging using the p:q tensor decomposition," *In submission, British Journal of Radiology*.
- [4] N. G. Kingsbury, "Image processing with complex wavelets," in *Phil. Transactions of London Royal Society*, 1999.
- [5] N. G. Kingsbury, "Complex wavelets for shift invariant analysis and filtering of signals," *Journal of Applied and Computational Harmonic Analysis*, vol. 10, 2001.
- [6] K. M. Hasan, P. J. Basser, D. L. Parker, and A. L. Alexander, "Analytical computation of the eigenvalues and the eigenvectors in DT-MRI," *Journal of Magnetic Resonance*, vol. 152, pp. 41–47, 2001.